

Weak localization in macroscopically inhomogeneous two-dimensional systems: a simulation approach

A. V. Germanenko,* G. M. Minkov, and O. E. Rut

Institute of Physics and Applied Mathematics, Ural State University, 620083 Ekaterinburg, Russia

(Dated: November 3, 2018)

A weak-localization effect has been studied in macroscopically inhomogeneous 2D system. It is shown, that although the real phase breaking length tends to infinity when the temperature tends to zero, such a system can reveal a saturated behavior of the temperature dependence of that parameter, which is obtained from the standard analysis of the negative magnetoresistance and usually identified by experimentalists with the phase braking length.

PACS numbers: 73.20Fz, 73.61Ey

The numerous experimental as well as theoretical papers are devoted to the weak localization in semiconductor structures and metal films. The problem was most intensively studied in the eightieth years. The theory of weak localization, which adequately describes experimental data, was developed. It gave simple analytical expressions for quantum correction to conductivity which allowed to determine a phase breaking time in real electron systems experimentally. The comprehensive review of the status of the problem at that time is given in Ref. 1,2.

In recent years the interest to this problem reappeared. One of the reason is that the new experimental results have been obtained. One of them is the saturation of the temperature dependence of the phase breaking time τ_φ .³ These papers cause a storm discussion in the literature (see, e.g., Refs. 5,6,7 and references therein) and stimulate a new flux of the papers concerning the weak localization.

A standard fitting procedure is used to analyze the experimental data and determine the phase breaking time practically in all cases: experimental magnetic-field dependencies of magnetoresistance are fitted to the theoretical ones,^{8,9} the phase breaking time is the fitting parameter.

Another approach to examination of the negative magnetoresistance due to weak localization has been presented in Ref. 10. It is based on a quasi-classical treatment of the problem^{11,12,13} and an analysis of the statistics of closed paths of a classic particle moving with scattering over 2D plane. This method has been applied to study the weak localization in InGaAs/GaAs heterostructures with single¹⁴ and double¹⁵ quantum wells.

The foregoing relates to homogeneous systems revealing only weak disorder on microscopic length scale. Of special interest are inhomogeneous systems, e.g., granular CuO films¹⁶ and percolating gold films.^{17,18,19} For interpretation of the experimental results the concept of anomalous diffusion is widely used. It should be mentioned that the transition from the weak localization to strong localization regime, when the system parameters or external conditions are varied, can also cross the macroscopically inhomogeneous state in originally homo-

geneous 2D systems.

In the present paper we analyze the weak-localization negative magnetoresistance in macroscopically inhomogeneous systems using approach developed in Ref. 10. The purpose is to show how the parameters, determined from the magnetoresistance experiments, match their real values in the systems with different inhomogeneity. Moreover, we show that this approach allows experimentally to distinguish what geometry of inhomogeneity is dominant in the system under investigation. As in Ref. 10 the results presented have been obtained from the numerical simulation of classical motion of particle.

We suppose that a macroscopically inhomogeneous 2D system consists of a number of puddles which are connected one with other by means of channels (Fig. 1(a)). The transport through the puddles and channels is diffusive, i.e. their dimensions are much greater than the mean free path of electrons. In this case the quasi-classical approach to consideration of the problem can be applied. We focus our attention on the case when the system is in inhomogeneous regime, i.e. when $L_\varphi < \xi_p$,²⁰ where ξ_p is the percolation correlation length, $L_\varphi = \sqrt{D\tau_\varphi}$, the diffusion constant is given by $D = v_F^2\tau/2$ with v_F as the Fermi velocity and τ representing the transport elastic mean-free time. Furthermore, we have idealized the situation and supposed that all the channels and puddles are identical, and our model system is a series-parallel connection of the elements, each of them is a channel and two half-puddles connected (Fig. 1(b,c)). We reduce thus the problem on the infinite inhomogeneous 2D system to the problem on the weak localization in one element, which is a diffusive constriction connecting two diffusive puddles. Because the channel and two paddles are connected in series, the correction to the conductance of the element is

$$\delta\sigma = \frac{1}{R_c + R_p} \left(\frac{R_c}{R_c + R_p} \frac{\delta\sigma_c}{\sigma_c} + \frac{2R_p}{R_c + R_p} \frac{\delta\sigma_p}{\sigma_p} \right), \quad (1)$$

where R_c , R_p are the resistances, σ_c , σ_p and $\delta\sigma_c$, $\delta\sigma_p$ are the conductivity and correction to the conductivity, respectively. Indexes c and p , hereafter, refer to the channel and puddle, respectively.

The quantities $\delta\sigma_c$ and $\delta\sigma_p$ are determined by the statistics of closed paths and can be found as

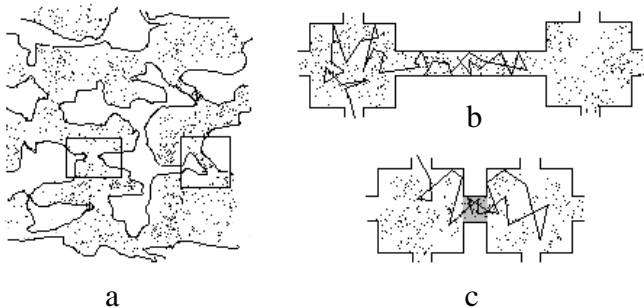


FIG. 1: (a) Sketch of inhomogeneous 2D system. The key parts determining the conduction are enclosed in rectangles. Non-conducting areas are white. Points represent scatterers. (b), (c) The models of long and square channels, respectively, used in simulation. Polygonal lines show particle trajectories. Shadowing in (c) shows the area with smaller value of the Fermi quasimomentum.

follows^{11,12,13}

$$\delta\sigma_{c,p} = -2\pi l^2 G_0 \mathcal{W}_{c,p} \quad (2)$$

where l denotes the mean-free path within the channel (l_p) or puddle (l_p), $G_0 = e^2/(2\pi^2\hbar)$, \mathcal{W} stands for the classical quasi-probability density for an electron to return to the start point within the channel (\mathcal{W}_c) or puddle (\mathcal{W}_p). With $\sigma = \pi k_F l G_0$, where k_F is the Fermi quasimomentum, we find

$$\delta\sigma = \frac{2}{\pi G_0 (R_c + R_p)^2} \left(\frac{K_c}{(k_F^c)^2} \mathcal{W}_c + 2 \frac{K_p}{(k_F^p)^2} \mathcal{W}_p \right), \quad (3)$$

where K_c and K_p are the length to width ratio of channel and puddle, respectively. Using formalism of Ref. 10, we can write for quasi-probabilities \mathcal{W}_c , \mathcal{W}_p in the presence of external magnetic field and inelastic scattering processes, destroying the phase coherence:

$$W_i(B) = \int_{-\infty}^{\infty} dS W_i(S) \exp\left(-\frac{\bar{L}_i}{l_\varphi^i}\right) \cos\left(\frac{2\pi BS}{\Phi_0}\right), \quad (4)$$

where $W_i(S)$ are the area distribution functions of closed paths, starting within the channel ($i = c$) or puddle ($i = p$), defined in such a way that $W_i(S)dS$ gives the classical probability density of return to the starting point with area enclosed S from the interval $(S, S + dS)$, $l_\varphi^i = v_F^i \tau_\varphi^i$, \bar{L}_i is the average length of closed paths with a given area, calculated by appropriate manner [Eq. (6) in Ref. 10], Φ_0 is the elementary flux quantum. Expressions (3) and (4) allow to obtain the magnetic field and temperature (through l_φ^i) dependence of conductance of our inhomogeneous model system.

Thus, the relative contributions of channel and puddles to the interference correction are determined not only by the statistics of closed paths, but geometry of channel

and puddles and the values of the Fermi quasimomentum in them.

In the present paper we consider the situation when the channel, which connects the square puddles ($K_p = 1$), mainly determines the conductance of whole 2D system and interference correction to it in actual range of parameters, i.e., the first term in Eq. (3) is greater than the second one. Two opposite cases are analyzed: (i) $k_F^c = k_F^p$, $K_c \gg 1$ (long channel); (ii) $k_F^c \ll k_F^p$, $K_c = 1$ (square channel). In the second case the lower value of the quasimomentum within the channel leads to arising of quasimomentum dependent reflection of electrons from the opened ends of channel. Those electrons, which attempt to enter the channel at an acute angle to the channel-puddle border ($\theta < \theta'$), are reflected and return to the puddle. All the electrons escaping the channel do this freely without any reflection. The value of θ' is determined by k_F^c to k_F^p ratio. The reflection can be specular, if the border is smooth, or diffusive, if the border is ragged. For simplicity we suppose that the border is straight line and reflection is specular.

Let us describe the simulation procedure. The element is represented as a lattice which contour corresponds to the geometry of element. The scatterers with given cross-section are placed in a part of lattice sites with the use of a random number generator. A particle is launched from some random point, then it moves with a constant velocity along straight lines, which happen to be terminated by collisions with the scatterers. After collision it changes the motion direction. If the particle collides with the walls of element, it is specularly reflected. If the particle passes near the starting point at the distance less than $d/2$ (where d is a prescribed value, which is small enough), the path is perceived as being closed. Its length and enclosed algebraic area are calculated and kept in memory. The particle walks over the element until it reaches one of the channel belonging to another element. As this happens one believes that the particle has left to infinity and will not return. A new start point is chosen and all is repeated.

The parameters used in simulation are the following: $d = 5$ [hereafter we measure length and area in units of lattice parameter and its square, respectively]; the number of launches $I_s = 10^5 \dots 10^6$; the length and width of channel are 4000 and 400 for long channel, 400 and 400 for square channel. The dimension of each puddle is 6000×6000 for all cases. The scattering is isotropic, the cross-section of the scatterers is equal to 7. The density of scatterers is such that the mean-free path is about 40 for both cases. For the case of square channel we use $(k_F^p/k_F^c)^2 = 10$, that gives the value of θ' about 70 degrees. For illustration, let us set the lattice parameter equal to 5 Å. Then our model provides an example of 2D system with local concentration of scatterers $1.5 \times 10^{12} \text{ cm}^{-2}$, $l = 200$ Å and $B_{tr} \simeq 0.8$ T, where $B_{tr} = \hbar c/(2el^2)$ is so called transport magnetic field.

We first turn to the area distribution function $W(S)$ (Fig. 2). The area range we are interested in is $S \gtrsim l^2$,

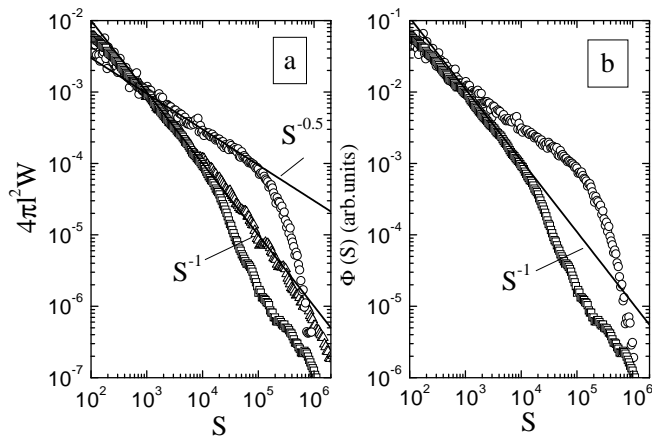


FIG. 2: (a) The area distribution functions $W_i(S)$ (a) and $\Phi(S)$ function (b). Symbols are the simulation results for the case of long (\circ), square (\square) channels, and for the paths starting within the puddle (\triangle). Only the positive area range is presented. Results obtained for negative algebraic areas are identical.

because just the long closed paths determine the low field negative magnetoresistance at low temperatures. As is seen, $4\pi l^2 W_p(S)$ mostly follows S^{-1} dependence. This is in agreement with the result of diffusion theory for infinite 2D system,^{10,21} which gives $4\pi l^2 W(S) = S^{-1} \tanh(\pi S/l^2) \simeq S^{-1}$ for $S > l^2$.

For the channels, the dependence $4\pi l^2 W(S)$ looks more complicated. For the long channels it is close to $S^{-0.5}$ -law within the area range $1 \times 10^3 - 5 \times 10^4$. It is precisely this behavior that is theoretically predicted for diffusive motion over infinitely long, narrow strip. A particular interest is drastic decrease of the area distribution function evident for $S > 10^5$. The origin is that the particle, moving along a long trajectory, reaches one of the ends of long channel, escapes the channel, and carries on the motion mainly within the puddles.

As for square channel, the $4\pi l^2 W_c$ -versus- S plot shows the behavior close to S^{-1} up to $S \simeq 10^4$, and reveals strong decrease at large areas as in previous case. This decrease is caused by the fact that a particle crosses the channel/puddle border freely only in one direction: when it moves from the channel to puddle. It cannot easily return back due to reflection from the opened ends of channel resulting from the difference of the Fermi quasi-momentum in channel and puddle discussed above.

In contrast to the area distribution functions, the dependencies $\bar{L}(S)$ are similar for all three cases.

In Figure 2 the function

$$\Phi(S) = \frac{K_c}{(k_F^c)^2} W_c(S) + 2 \frac{K_p}{(k_F^p)^2} W_p(S), \quad (5)$$

which determines the magnetic field dependence of interference quantum correction of the element, is plotted. Namely this function rather than the area distribution function as in homogeneous 2D case will be obtained

when the approach to analysis of the negative magnetoresistance suggested in Refs. 10 is applied. As is seen the Φ -versus- S curve shows more rapid than S^{-1} decreasing in wide area range for both cases considered.

We turn now to consideration of the interference quantum correction to the conductivity. It has been found using Eq. (3) and discrete form of Eq. (4) [see Ref. 10 for details]:

$$W_i = \frac{1}{I_s d l} \sum_k \cos\left(\frac{b S_k}{l^2}\right) \exp\left(-\frac{l_k}{l_\varphi}\right), \quad i = c, p. \quad (6)$$

Here, summation runs over all closed paths, S_k , l_k are the area enclosed and the length of k th closed path, respectively, b is magnetic field measured in units of B_{tr} . Deriving Eq. (6) we have supposed that τ_φ is the same within the channel and puddles. In this case W_i are independent of the Fermi velocity v_F . Figure 3(a) shows the simulation results for $\delta\sigma(b=0)$, obtained for different l/l_φ values, and, for comparison, the results of theoretical calculation obtained through the well-known formulas^{1,6}

$$\delta\sigma = -G_0 \ln\left(1 + \frac{l_\varphi}{l}\right) \quad (7)$$

for 2D case, and

$$\delta\sigma = -6.094 G_0 L_c^{-1} \sqrt{l_\varphi l} \quad (8)$$

for quasi one-dimensional case with L_c as channel length. As is seen the simulation results reveal the behavior close to theoretical ones only for considerably large l to l_φ ratios: $l/l_\varphi > 0.01$. Experimentally, this corresponds to the high temperatures. With lowering l/l_φ , i.e., with temperature decrease, the simulation data tend to saturate as opposed to the theories. It is clear that such a behavior is a result of steep fall in $\Phi(S)$ dependencies at large areas (see Fig. 3(b)).

Let us analyze the magnetic field dependencies of interference quantum correction. As an example, in Fig. 3(b) we present the dependencies $\Delta\sigma(b) = \delta\sigma(b) - \delta\sigma(0)$ calculated with $l/l_\varphi = 3.5 \times 10^{-3}$. We have considered these data as experimental ones and fitted them to the well-known expression^{8,9}

$$\Delta\sigma(b) = a G_0 \left[\psi\left(\frac{1}{2} + \frac{\gamma}{b}\right) - \psi\left(\frac{1}{2} + \frac{1}{b}\right) - \ln \gamma \right], \quad (9)$$

where $\psi(x)$ is a digamma function. The parameters a and $\gamma = l/l_\varphi$ have been used as fitting ones. Just this procedure is usually used to determine the value of l_φ in real 2D samples. Results of the fit are represented in Fig. 3(b) by curves. As is seen, Eq. (9) satisfactorily describes the simulation data.

How the value of γ , found from the fitting, matches the value of $l/l_\varphi = \tau/\tau_\varphi$, put in Eq. (6), is shown in Fig. 4(a). The fitting procedure gives the value of γ which is less than the value of l/l_φ . In the case of square channel, l/l_φ -dependence of γ can be described by the power function:

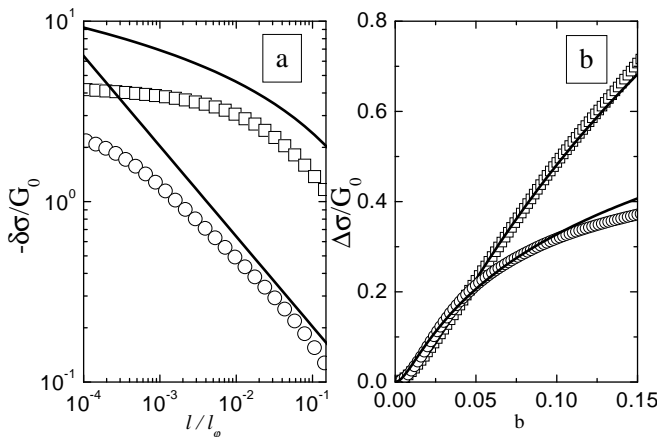


FIG. 3: (a) The interference quantum correction to the conductivity in zero magnetic field as a function of l/l_φ obtained from the simulation (symbols), calculated from Eq. (7) (upper curve) and Eq. (8) (lower curve). (b) The magnetic field dependence of interference quantum correction to the conductivity obtained from the simulation with $l/l_\varphi = 3.5 \times 10^{-3}$ (symbols). Curves are the best fit to Eq. (9), carried out for $b \leq 0.1$. Symbolic designations are the same as in Fig. 2.

$\gamma \propto (l/l_\varphi)^{0.8}$. As for the case of long channel, the γ -versus- l/l_φ plot shows saturation at $l/l_\varphi < 10^{-3}$. On the assumption of $l_\varphi \propto T^{-\alpha}$, $\alpha > 0$, Figure 4(a) shows qualitative temperature dependencies of the “phase breaking time” as it is obtained from the standard fitting procedure. Thus, the presence of macroscopical inhomogeneity in samples can lead to inconsistency between temperature dependence of the “phase breaking time”, found experimentally, and the real temperature dependence of τ_φ . This inconsistency may be qualitative for inhomogeneous samples in which the conduction through the long channels dominates: the value obtained from the fitting procedure can be saturated, whereas the real phase breaking time decreases with decrease of temperature and diverges at $T \rightarrow 0$. Using quota we underline that the “phase breaking time” is nothing more than the fitting parameter here. It should not be always identified with the real value of phase breaking time.

Finally, we present the l/l_φ -dependence of prefactor a (Fig. 4(b)). Absolute value of a has no meaning, because its value should depend on size distribution of channels in real sample. However, the dependence is meaningful. In both cases considered the value of prefactor a strongly depends on l to l_φ ratio, and the direction of change of a with growing l/l_φ is determined by the kind of inhomogeneity: for long channel, the value of a increases with decrease of l/l_φ , whereas it decreases for the case of square channel.

Note, that the results presented cannot be extrapolated down to $l/l_\varphi = 0$ [or $T = 0$]. The point is that for $l/l_\varphi < 2 \times 10^{-5}$ the value of $L_\varphi = \sqrt{l_\varphi l}$ becomes greater than the size of the element, which determines the correlation length ξ_p . In this case our system should

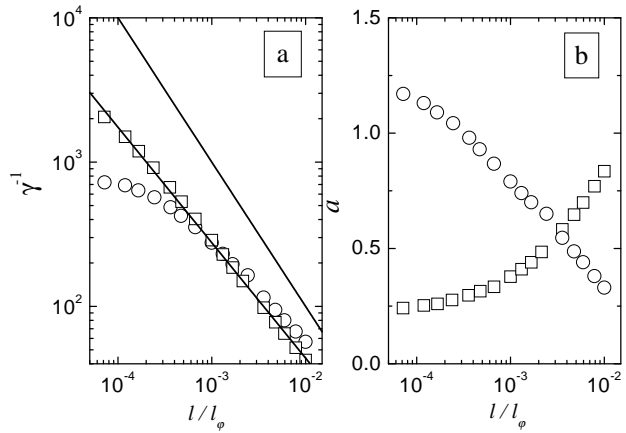


FIG. 4: The fitting parameters γ (a) and a (b) as function of l/l_φ ratio. Upper line in (a) is $\gamma = l/l_\varphi$, lower is $\gamma \propto (l/l_\varphi)^{0.8}$. Symbolic designations are the same as in Fig. 2.

behave itself as homogeneous one. Thus, it seems reasonable to say that the l/l_φ -dependence of γ must tend to $\gamma \propto l_\varphi^{-1}$, and the value of prefactor must be equal to unity for $L_\varphi \gg \xi_p \simeq 10^4$.

In conclusion, we have numerically studied the statistics of closed paths and the negative magnetoresistance in macroscopically inhomogeneous 2D systems. We have considered the situation when the main contribution to the quantum interference correction to the conductivity comes from constrictions. Two types of constrictions have been considered: long and square channels. We have shown that the magnetic field dependence of the negative magnetoresistance is well fitted to the Hikami expression for both systems. However, the value of the fitting parameter γ does not coincide with the value l/l_φ fed into simulation, and, moreover, the γ -versus- l/l_φ plot is not linear. This means that the temperature-dependence of the “phase breaking time”, as it is obtained experimentally from the standard analysis of the negative magnetoresistance for inhomogeneous 2D system, can differ drastically from the real temperature dependence of τ_φ . An indicator, whether the system is inhomogeneous, is the strong temperature dependence of the prefactor. The Fourier transformation of the magnetic field dependencies of the negative magnetoresistance taken at different temperatures^{10,14,15} can be used in order to obtain the function $\Phi(S)$, which carries direct information about the area distribution function of closed paths, and, consequently, about the character of inhomogeneity of the samples, investigated.

The results presented can be directly used to interpret the weak-localization experiments carried out on the artificial diffusive cavities and constrictions. To our knowledge there is deficit of the paper devoted to such objects. The main attention was attracted to the ballistic cavities and systems with antidot arrays [see, for example, Ref. 22].

The authors are grateful to I. V. Gornyi for many valu-

able discussions. This work was supported in part by the RFBR through Grants No. 00-02-16215 and No. 01-02-17003, the Program *University of Russia* through Grants

No. 990409 and No. 990425, and the CRDF through Award No. REC-005.

-
- * Electronic address: Alexander.Germanenko@usu.ru
- ¹ B. L. Altshuler, and A. G. Aronov, in *Electron-Electron Interaction in Disordered Systems*, edited by A. L. Efros and M. Pollak, (North Holland, Amsterdam, 1985) p.1.
 - ² P. A. Lee and T. V. Ramakrishnan, *Rev. Mod. Phys.*, **57**, 287 (1985), G. Bergman, *Physics Reports*, **107**, 1 (1984), B. L. Altshuler, A. G. Aronov, D. E. Khmel'nitski, and A. I. Larkin, in *Quantum theory of solids*, edited by I. M. Lifshitz, (Mir Publishers, Moscow, 1982).
 - ³ P. Mohanty, E. M. Q. Jarivala, and R. A. Webb, *Phys. Rev. Lett.* **78**, 3366 (1997), P. Mohanty and R. A. Webb, *Phys. Rev. B* **55**, 13452 (1997), C. Prasad, D. K. Ferry, A. Shailos, M. Elhassen, J. P. Bird, L.-H. Lin, N. Aoki, Y. Ochiai, K. Ishibashi, and Y. Aoyagi, *Phys. Rev. B* **62**, 15356 (2000).
 - ⁴ M. E. Gershenson, *Annalen der Physik* **8**, 559 (1999).
 - ⁵ B. L. Altshuler, M. E. Gershenson, and I. L. Aleiner, *Physica E* **3**, 58 (1998), B. L. Altshuler, I. L. Aleiner, and M. E. Gershenson. *Phys. Rev. Lett.* **82**, 3190 (1999).
 - ⁶ I. L. Aleiner, B. L. Altshuler, and M. E. Gershenson. *Waves in Random Media* **9**, 201 (1999).
 - ⁷ Dmitrii S. Golubev, and Andrei D. Zaikin, *Phys. Rev. B* **59**, 9195 (1999), *Phys. Rev. B* **62**, 14061 (2000).
 - ⁸ S. Hikami, A. Larkin and Y. Nagaoka, *Prog. Theor. Phys.* **63**, 707 (1980).
 - ⁹ H.-P. Wittman and A. Schmid, *J. Low. Temp. Phys.* **69**, 131 (1987).
 - ¹⁰ G. M. Minkov, A. V. Germanenko, O. E. Rut, and I. V. Gornyi, *Phys. Rev. B* **61**, 13164 (2000).
 - ¹¹ S. Chakravarty and A. Schmid, *Phys. Reports* **140**, 193 (1986).
 - ¹² M. I. Dyakonov, *Solid St. Comm.* **92**, 711 (1994).
 - ¹³ I. V. Gornyi, A. P. Dmitriev, and V. Yu. Kachorovskii, *Phys. Rev. B* **56**, 9910 (1997).
 - ¹⁴ G. M. Minkov, S. A. Negashev, O. E. Rut, A. V. Germanenko, O. I. Khrykin, V. I. Shashkin, and V. M. Danil'tsev, *Phys. Rev. B* **61**, 13172 (2000).
 - ¹⁵ G. M. Minkov, A. V. Germanenko, O. E. Rut, O. I. Khrykin, V. I. Shashkin and V. M. Danil'tsev, *Phys. Rev. B* **62**, 17089 (2000).
 - ¹⁶ A. G. Aronov, M. E. Gershenson, and Yu. E. Zhuravlev, *Zh. Eksp. Teor. Fiz.*, **87** 971 (1984) [*Sov. Phys. JETP* **60**, 554 (1984)].
 - ¹⁷ A. Palevskii and G. Deutscher, *Phys. Rev. B* **34**, 431 (1986).
 - ¹⁸ G. Dumpich and A. Carl, *Phys. Rev. B*, **43** 12074 (1991).
 - ¹⁹ S. Friedrichowski, A. Carl, and G. Dumpich, *Europhys. Lett.*, **32**(3), 247 (1995).
 - ²⁰ D. Stauffer, *Introduction to Percolation Theory* (Taylor & Francis, London, 1985).
 - ²¹ K. V. Samokhin, *Phys. Rev. E* **59**, R2501 (1999).
 - ²² I. L. Aleiner and A. I. Larkin, *Phys. Rev. B* **54**, 14423 (1996), Bodo Huckestein, Roland Ketzmerick, Caio H. Lewenkopf, *Phys. Rev. Letters* **84**, 5504 (2000).